

---

# A Universal Hierarchy of Shift-Stable Distributions and the Tradeoff Between Stability and Performance

---

**Adarsh Subbaswamy**  
Johns Hopkins University  
asubbaswamy@jhu.edu

**Bryant Chen**  
Brex\*  
bryant@brex.com

**Suchi Saria**  
Johns Hopkins University  
ssaria@cs.jhu.edu

## Abstract

Many methods which find invariant predictive distributions have been developed to learn models that can generalize to new environments without using samples from the target distribution. However, these methods consider differing types of shifts in environment and have been developed under disparate frameworks, making their comparison difficult. In this paper, we provide a unifying graphical representation of the data generating process that can represent all such shifts. We show there is a universal hierarchy of shift-stable distributions which correspond to operators on a graph that disable edges. This provides the ability to compare current methods and derive new algorithms that find optimal invariant distributions, all of which can be mapped to the hierarchy. We theoretically and empirically show that the degree to which stability is desirable depends on how concerned we are about large shifts: there is a tradeoff between stability and average performance.

## 1 Introduction

Increasing deployment of machine learning models in high impact applications such as healthcare (Henry et al., 2015; Yu et al., 2018) and criminal justice (Lum and Isaac, 2016) has led to renewed emphasis on improving and ensuring their *safety* and *reliability* (Amodei et al., 2016; Saria and Subbaswamy, 2019). To do so, developers are forced to reason in advance about likely sources of failure and address them prior to deployment. One source of failure is due to *shifts in environment* between the environment in which training data was collected and the environment in which the model will be deployed. In cases where data from the deployment environment is unavailable, failing to account for the differences can result in dangerous decisions and worse performance than anticipated.

For example, Caruana et al. (2015) consider a case in which a model was trained to predict mortality ( $M$ ) due to pneumonia ( $P$ ) using data from hospitalized patients. The motivation of the original study (Cooper et al., 1997) was to deploy the model for triage—to determine whether or not to admit patients—representing a shift to a new environment in which the patients have not yet been hospitalized. In this case, the model learned an *unstable* association in the source environment that does not hold in the deployment environment: it learned that patients with asthma ( $A$ ) were less likely to die because of admission policy since asthmatic patients were more likely to be directly admitted to the ICU ( $I$ ) at the hospital. In the deployment environment the patients have not been admitted to the hospital (i.e., admission policy is different) and thus the model makes dangerously incorrect predictions that asthmatic patients have lower risk of mortality.

---

\*Much of this work was conducted while at IBM Research AI

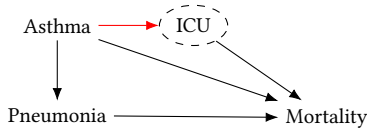


Figure 1: Posited graph for the pneumonia example of Caruana et al. (2015). The red edge represents the unstable relationship while the dashed node represents an unobserved variable.

In recent work addressing such shifts in environment, Subbaswamy et al. (2019) provided a graphical language for expressing shifts that are likely to occur. They explicitly represent the underlying data generating process (DGP) with a graph of causal mechanisms (directional knowledge of causes and effects) relating the variables in a prediction problem. The graph is augmented to identify the pieces of the DGP (i.e., conditional distributions encoding mechanisms) that are unstable and can vary across environments. A graph of the DGP in the pneumonia example is given in Fig 1, in which the unstable edge (red) encodes the varying association due to ICU admission policy  $P(I|A)$ . To prevent failures due to anticipated shifts in environment, methods for addressing the shifts seek to find *stable* distributions that are invariant to arbitrary changes in the unstable conditionals.<sup>2</sup> In this case, had ICU status been observed  $P(M|P, A, I)$  is a stable distribution that could be used to make predictions that are invariant to differences in ICU admission policy (Schulam and Saria, 2017; Subbaswamy et al., 2019).

These shifts happen in nearly every domain where machine learning is deployed, since the data were generated according to some process. The importance of the explicit graphical representation of the DGP is to allow us to identify and express the pieces of the DGP we want to guard against shifts.<sup>3</sup> However, in broader contexts than reliability, prior work has considered the problem of making invariant predictions that generalize to new, unseen environments, with a number of methods using heterogeneous data from multiple source environments to empirically find stable distributions which are invariant to the shifts (Peters et al., 2016; Rojas-Carulla et al., 2018; Magliacane et al., 2018; Kuang et al., 2018). Additionally, other work has considered specific types of shifts, such as mean-shifts in mechanisms (Rothenhäusler et al., 2018) or shifts in edge strengths (Subbaswamy and Saria, 2018).

While various methods developed in disparate frameworks all find stable distributions, we will unify them by showing there are three types of stable distributions that relate to the graph underlying a prediction problem. We do this by developing a novel graphical representation of shifts that extends prior work which represents shifts in mechanisms (Pearl and Bareinboim, 2011; Subbaswamy et al., 2019). Through this representation we can analyze the effects of using stable distributions to predict on performance across environments. Relatedly, many works have either demonstrated or proved that when the shifts are arbitrarily strong, an unstable model will perform worse in the target environment than a stable model with respect to *minimax risk*—worst-case expected loss across possible environments. In contrast, we additionally show there is a tradeoff between stability and performance in the average environment which affects the choice of whether or not to use a stable model.

**Contributions:** Motivated by the need for models that can accurately predict in new environments, many methods have been developed which find distributions that are stable to various types of shifts in environment. However, these methods have been developed in disparate frameworks that make it difficult to compare different stable solutions. In this paper, we provide a unifying framework for different types of shifts and stable solutions. We create a novel graphical representation for arbitrary-strength shifts of different types in terms of edges in the graph (Definition 4). This representation encompasses shifts that have been previously considered, and is extensible to other types of shifts. Further, we show that *all stable distributions correspond to distributions which disable unstable edges in the graph* (Theorem 1), thereby unifying the disparate frameworks. We also develop a hierarchy of stable distributions which correspond to three types of operators on the graph that differ in how precisely they disable edges (Corollary 2). This establishes the notion of an optimal stable distribution, providing for the first time a way to compare different stable solutions. Finally, we analyze the effect of disabling edges on performance across possible

<sup>2</sup>We will refer to distributions that are stable to shifts in environment as “shift-stable” or simply “stable”.

<sup>3</sup>In practice, the graph may not be fully known. *Structure learning* (Spirtes et al., 2000) could be used to learn a graphical equivalence class from data; we could consider the sensitivity of solutions across the equivalence class.

environments, demonstrating that there is a tradeoff between stability and average performance in environments. We explore this tradeoff in simulated and real data to show that stable models conservatively minimize worst-case performance while unstable models can perform better on average.

## 2 Related Work

Traditional approaches for addressing dataset shift typically assume access to unlabeled samples from the target distribution, which they use to reweight training data during learning (see, e.g., Quiñero-Candela et al. (2009) for an overview). However, when the target environment is unknown (such as in the context of reliability) we require *proactive* methods that learn without requiring samples from the target environment (Subbaswamy and Saria, 2018). Proactive methods make assumptions about the set of possible target environments in order to be able to learn a model from source environment data that can be applied elsewhere. In this paper we focus on shifts of arbitrary strengths, though others have considered how to make predictions with *bounded magnitude distributional robustness* (e.g., Sinha et al. (2017); Heinze-Deml and Meinhäuser (2017)). Most relevant to this work, Rothenhäusler et al. (2018) consider bounded mean-shifts in mechanisms but show that for unbounded strength mean-shifts the solution reduces to a stable distribution.

Another class of proactive methods is entirely data-driven approaches which use data from multiple source environments. They are motivated by the observation that, assuming there are no shifts to the target prediction variable itself, the distribution of a variable given all of its parents in a causal graph is invariant to arbitrary shifts in all other variables (including its parents). This is known as the “independence of cause and mechanism” (Peters et al., 2017) which, in the case of no unobserved variables, has led to methods for *causal discovery* that empirically determine the causal relationships using data from multiple environments (Peters et al., 2016; Heinze-Deml et al., 2018). Leveraging this for the purposes of invariant prediction, recent works employ similar techniques to find an invariant subset of features  $X$  that yield a stable conditional distribution  $P(Y|X)$  that can be used to predict (Rojas-Carulla et al., 2018; Magliacane et al., 2018). For settings in which data from only one source environment are available, Kuang et al. (2018) use covariate balancing techniques to determine the causal features that yield a stable conditional.

These methods all make assumptions about types of graphs underlying the data they are applied to, such as assumptions about the existence of unobserved confounders or the existence of a stable feature set. In contrast, other methods assume explicit knowledge of the graph representing the DGP. Given additional knowledge of the mechanisms that are expected to vary across environments, these methods return a stable distribution if it exists. They not only consider conditional distributions, but also interventional (Subbaswamy et al., 2019) and counterfactual distributions (Subbaswamy and Saria, 2018). Notably, Subbaswamy et al. (2019) use *selection diagrams* (Pearl and Bareinboim, 2011) to identify mechanisms that can shift. In Section 3 we will develop an edge-based representation for shifts of arbitrary types, that in some cases is more expressive in that it identifies the particular edge in a mechanism that is unstable.

## 3 A Causal Hierarchy of Shift-Stable Distributions

We first introduce necessary background on causal graphs before defining stability and the types of shifts in mechanism previously considered. We then develop a unifying graphical representation for expressing arbitrary-strength shifts of different types, and provide a graphical criterion for determining the stability of a distribution. We present a universal hierarchy of stable distributions, relating existing methods, and show increasing levels of the hierarchy have increasing precision in disabling unstable edges. Motivated by these findings, in Section 4 we will investigate how disabling edges interacts with performance across environments. Proofs of results are in the supplement.

### 3.1 Preliminaries

**Notation** Throughout the paper sets of variables are denoted by bold capital letters while their particular assignments are denoted by bold lowercase letters. We will consider graphs with directed or bidirected edges (e.g.,  $\leftrightarrow$ ). Acyclic will be taken to mean that there exists no purely directed cycle. The sets of parents, children, ancestors, and descendants in a graph  $G$  will be denoted by

$pa_{\mathcal{G}}(\cdot)$ ,  $ch_{\mathcal{G}}(\cdot)$ ,  $an_{\mathcal{G}}(\cdot)$ , and  $deg_{\mathcal{G}}(\cdot)$ , respectively (subscript  $\mathcal{G}$  omitted when obvious from context). For an edge  $e$ ,  $He(e)$  and  $Ta(e)$  will refer to the head and tail of the edge, respectively.

**Structural Causal Models** We will represent the data generating process (DGP) underlying a prediction problem using a graph,  $\mathcal{G}$ , which consists of a set of vertices  $\mathbf{O}$  corresponding to observed variables and sets of directed and bidirected edges such that there are no directed cycles. Directed edges indicate direct causal effects while bidirected edges indicate the presence of an unobserved confounder (common cause) of the two variables. The prediction problem associated with the graph consists of a target output variable  $Y$  and the remaining observed variables as input features.

The graph  $\mathcal{G}$  defines a Structural Causal Model (SCM) (Pearl, 2009) in which each variable  $V_i \in \mathbf{O}$  is generated as a function of its parents and its variable-specific exogenous noise variable  $U_i$ :  $V_i = f_i(pa(V_i), U_i)$ . For our performance analysis we will consider linear Gaussian SCMs which can be expressed as a set of equations  $\mathbf{O} = \Lambda \mathbf{O} + \mathbf{U}$ .  $\Lambda$  can be arranged as a lower triangular matrix of structural coefficients associated with directed edges in  $\mathcal{G}$  and  $\mathbf{U}$  are the multivariate Gaussian distributed exogenous variables with covariance matrix  $\mathcal{E}$ . Nonzero off-diagonal elements of  $\mathcal{E}$  correspond to bidirected edges in  $\mathcal{G}$ . The covariance matrix of linear Gaussian SCMs decomposes as  $\Sigma = (I - \Lambda)^{-T} \mathcal{E} (I - \Lambda)^{-1}$ , a property we will exploit in our analysis of performance. We will further assume that all variables are mean 0.

### 3.2 Stability and Types of Shifts

In this section we introduce the relevant types of shifts before graphically defining instability in terms of edges. To define the shifts, assume that there is a set of environments such that a prediction problem maps to the same graph structure  $\mathcal{G}$ . However, each environment is a different instantiation of that graph such that certain mechanisms differ. One example was Fig 1, in which the graph was the same in both environments but the ICU admission policy was different. As another simple example, consider the graph in Fig 2a. Suppose we wanted to diagnose pneumonia  $Y$  from chest X-rays  $Z$  and stylistic features (i.e., text, orientation, coloring) of the image  $X$ . The latent variable  $W$  represents the hospital department the patient visited. Because each department has its own protocols and equipment, the style preferences  $P(X|W)$  vary across departments. Since in this case  $W$  is not recorded, a model of  $P(Y|X, Z)$  will learn an association between  $Y$  and  $Z$  through  $W$ , so pneumonia predictions will be unreliable in new departments or when equipment/protocols change. This is a case in which we desire invariance to *arbitrary shifts* in the style mechanism  $P(X|W)$ .

**Definition 1** (Arbitrary shifts in mechanism). An arbitrary shift in the mechanism generating a variable  $V$  corresponds to arbitrary shifts in the distribution  $P(V|pa(V))$ .

This is the most common and general shift considered in prior work (Peters et al., 2016; Rojas-Carulla et al., 2018; Magliacane et al., 2018; Kuang et al., 2018; Subbaswamy et al., 2019). For methods that do not assume the graph is known, they assume there exists a subset of features  $\mathbf{X}$  such that  $P(Y|\mathbf{X})$  is stable to arbitrary shifts in the mechanisms of all variables except  $Y$ . *Mean-shifted mechanisms* are a special case that has also been studied (Meinshausen, 2018; Rothenhäusler et al., 2018).

**Definition 2** (Mean-shifted mechanisms). An (arbitrary) mean-shift in the mechanism generating a variable  $V$  corresponds to an environment-specific (arbitrary) change in the intercept of its linear structural equation  $V = \text{intercept}_{env} + \sum_{X \in pa(V)} \lambda_{xv} X + u_v$ .

Subbaswamy and Saria (2018) speak of shifts in mechanism, but their method can actually deal with another special case: *edge-strength shifts* in which a subset of edges into a variable may vary.

**Definition 3** (Edge-strength shift). An edge-strength shift in edge  $X \rightarrow V$  corresponds to a change in the *natural direct effect*: for  $Y = pa(V) \setminus X$  we have that  $E[V(x'), Y(x)] - V(x)$  changes, where  $V(x)$  is the counterfactual value of  $V$  had  $X$  been  $x$ .

**Key Result:** *All of these shifts can be expressed in terms of edges.* First, edge-strength shifts naturally correspond to particular edges. Next, since the mechanism generating a variable  $V$  is encoded graphically by all of the edges into  $V$ , shifts in mechanism can also be represented by marking all edges into  $V$ .<sup>4</sup> Finally, mean-shifts correspond to an edge  $A \rightarrow V$  where for environment (or

<sup>4</sup>For shifts in mechanism to an exogenous variable  $V$  with no parents in the graph, one might imagine adding an explicit mechanism variable  $M_V$  to the graph and considering the edge  $M_V \rightarrow V$  to be unstable.

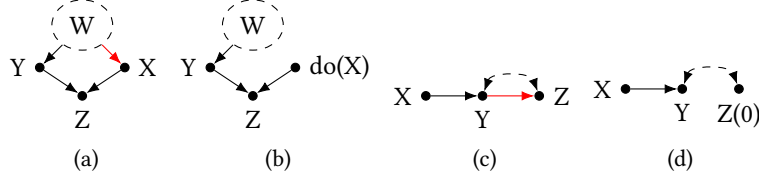


Figure 2: (a) Graph where a level 1 distribution imprecisely disables edges. (b) Level 2 operator applied to (a). (c) Graph where level 2 distribution imprecisely disables edges. (d) Level 3 operator applied to (c). Red edges are unstable. Dashed node is latent.

“anchor”) A the mean of  $V$  is shifted. We will denote the set of *unstable edges* that can vary across environments as  $E_u \subseteq E$  where  $E$  is the set of edges in  $\mathcal{G}$ . Graphically, unstable edges will be colored.

**Definition 4** (Unstable Edge). An edge is said to be unstable if it is the target of an edge-strength shift or the mechanism associated with the edge is the target of an arbitrary shift.

We can now define *stable distributions*, which are the target of estimation for the methods addressing instability due to shifts. A *stable predictor* will be a model of a stable distribution.

**Definition 5** (Stable Distribution). A distribution  $P(Y|Z)$  is said to be a stable if for any two environments  $\mathcal{G}_1$  and  $\mathcal{G}_2$  that are instantiations of the same graph  $\mathcal{G}$ ,  $P_{\mathcal{G}_1}(Y|Z) = P_{\mathcal{G}_2}(Y|Z)$  holds.

Having established a common graphical representation for arbitrary shifts of various types, we provide a graphical definition of stable distributions. First, define an active *unstable path* to be an active path (as determined by the rules of  $d$ -separation (Pearl, 1988)) that contains at least one unstable edge. **Key Result:** *The non-existence of unstable paths is a graphical criterion for determining a distribution’s stability.*

**Theorem 1.**  $P(Y|Z)$  is stable if there is no active unstable path from  $Z$  to  $Y$  in  $\mathcal{G}$  and the mechanism generating  $Y$  is stable.

In the next section we use the graphical characterization provided by Theorem 1 to show all stable distributions, including those found by existing methods, can be categorized into three levels.

### 3.3 Hierarchy of Shift-Stable Distributions

We established that instability in a graph corresponds to unstable edges, and that stable distributions are those that do not make use of associations containing unstable edges. We now introduce a universal hierarchy of the 3 categories of stable distributions: 1) observational conditionals, 2) conditional interventionals, and 3) counterfactuals.<sup>5</sup> The hierarchy establishes when stability to shifts is achievable, and shows that different levels correspond to operators which differ in the precision with which they can disable edges (Corollary 2, main result of this subsection).

Methods at level 1 of the hierarchy seek invariant conditional distributions of the form  $P(Y|Z)$  that use a subset of observed features for prediction (Peters et al., 2016; Rojas-Carulla et al., 2018; Magliacane et al., 2018; Kuang et al., 2018). These distributions only have conditioning (i.e., the standard rules of  $d$ -separation) as a tool for disabling unstable edges. *The conditioning operator is coarse and removes large pieces of the graph.* Consider Figure 2a, with prediction target  $Y$ . The only stable level 1 distribution is  $P(Y)$ , since conditioning on either of the observed variables  $X$  or  $Z$  activates the path through the unstable (red) edge. Thus, in this graph, the conditioning operator disables all paths from  $X$  and  $Z$  to  $Y$ , including stable paths.

Methods at level 2 (Subbaswamy et al., 2019) find conditional interventional distributions (Pearl, 2009) of the form  $P(Y|do(\mathbf{W}), Z)$ . In addition to conditioning, level 2 distributions use *the do operator, which deletes all edges into an intervened variable.* Fig 2b shows the result of  $do(X)$  applied to Fig 2a: the edges into  $X$  (namely the unstable edge) are removed. Thus,  $P(Y|Z, do(X))$  is stable and retains statistical information along stable paths from  $Z$  and  $X$  that the level 1 distribution  $P(Y)$  did not. In Fig 2c, however, applying  $do(Z)$  yields the graph  $X \rightarrow Y$ , and edges into  $Z$ , including the stable  $\leftrightarrow$  edge, would be removed.

<sup>5</sup>This is related to the hierarchies of causal queries (Pearl, 2009) and interventions (Shpitser and Tchetgen, 2016).

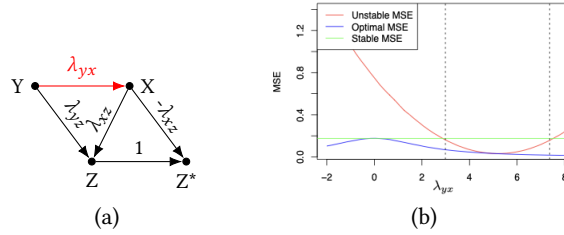


Figure 3: (a) Example with the AV  $Z^*$ .  $P(Y|Z^*)$  is the optimal stable level 3 distribution. (b) Oracle and stable MSEs as  $\lambda_{yx}$  varies.

Finally, level 3 methods (Subbaswamy and Saria, 2018) seek distributions corresponding to counterfactuals. Counterfactuals allow us to consider conflicting values of a variable. For example, let  $Y$  and  $Z$  denote two children of a variable  $X$ . If we hypothetically set  $X$  to  $x'$  for  $X \rightarrow Y$  but left  $X$  as its observed value  $x$  for  $X \rightarrow Z$ , this corresponds to counterfactual  $Y(x')$  and factual  $Z(x) = Z$ . By setting a variable to a reference value (e.g., 0) for one edge but not others, *computing counterfactuals can effectively remove a single edge*. In Fig 2c, we saw that  $P(Y|X, do(Z))$  is stable and deletes both edges into  $Z$ . However, if we compute the counterfactual  $Z(Y = 0)$ , resulting in Fig 2d, then the level 3 distribution  $P(Y|X, Z(Y = 0))$  is stable and only deletes the unstable  $Y \rightarrow Z$  edge, retaining information along the  $Y \leftrightarrow Z$  path. The next result follows from the effects of the three operators:

**Corollary 2.** *Distributions at increasing levels of the hierarchy of stability grant increased precision in disabling individual edges (and thus paths).*

**Key Result:** *Thus, the difference between operators associated with the different levels of stable distributions is the precision of their ability to delete edges into a variable.* Level 1, conditioning, must remove large amounts of the graph to disable edges. Level 2, intervening, deletes all edges into a variable. Level 3, computing counterfactuals, can precisely delete a single edge into a variable. Since paths encode statistical influence, this also provides a natural definition for an *optimal stable distribution* as one which deletes the unstable edges, and only the unstable edges. Thus, given a stable distribution found by any method, we can compare to the optimal stable distribution to see which, and how many, stable paths were removed.

Another important fact is that the hierarchy is *nested*:

**Lemma 3** (Subbaswamy et al. (2019), Corollary 1). *A stable level 1 distribution of the form  $P(Y|Z)$  can be expressed as a stable level 2 distribution of the form  $P(Y|Z', do(W))$  for  $Z' \subseteq Z \subseteq O$ ,  $W \subseteq O$ .*

**Lemma 4.** *A stable level 2 distribution of the form  $P(Y|Z', do(W))$  can be expressed as a stable level 3 distribution of the form  $P(Y(W)|Z'(W))$ .*

**Consequences:** A significant consequence of the hierarchy of shift-stable distributions is that it determines when it is possible to achieve invariance to shifts. Since the hierarchy is nested, we know that if there are no stable level 2 or 3 distributions, then there is no stable level 1 distribution. Considering the other direction, if we find that no stable conditional distribution exists, this does not mean that we cannot achieve stability: stable level 2 or 3 distributions may still exist. This motivates future work that considers distributions at the highest levels of the hierarchy. However, there is a caveat: the highest level distributions may not be *identifiable*—they cannot always be estimated as a function of the observational training data. This is as opposed to level 1 distributions, which can always be learned from training data. Further, estimation of counterfactuals requires assumptions (additional to identifiability assumptions required for level 2) about the functional form of the SCM (see Pearl (2009, Chapter 7)).

We have shown that the hierarchy of stable distributions establishes possibility results for achieving stability to shifts, and that all stable distributions correspond to disabling or removing edges in the the underlying graph. In the next section, we investigate the effect of edge removal on prediction performance across environments.

## 4 On the Performance of Stable Distributions

In the previous subsection we established that methods for stable prediction achieve stability through hypothetical deletions of edges in the graph underlying a prediction problem. In this

section we examine how the strength of a deleted edge affects the relative performance of stable model. This provides useful insights because, in general, it is possible to learn edge strengths from data. To facilitate the analysis, we will consider linear SCMs and quantify how far a stable distribution is from achieving the highest achievable performance in a given environment (defined by edge strength). Note that in any given environment the optimal predictor (w.r.t. mean squared error (MSE)) is the conditional expectation  $E[Y|\mathbf{O}]$  (Friedman et al., 2001). Thus, we will define the *regret* associated with a given environment to be the difference in performance between a stable predictor and the *oracle* conditional expectation in that environment.

We will consider the form of a level 3 stable distribution since they generalize all stable distributions (Lemma 4) and have the greatest precision in removing singular edges (Corollary 2):  $P(Y|\mathbf{W}^*, \mathbf{Z})$ , where  $\mathbf{Z} \subseteq \mathbf{O}$  consists of observed variables and  $\mathbf{W}^* \cap \mathbf{O} = \emptyset$  consists of counterfactual versions of observed variables (Subbaswamy and Saria, 2018). This means the only difference between a level 3 stable predictor ( $E[Y|\mathbf{W}^*, \mathbf{Z}]$ ) and an oracle predictor is the feature set. Thus, regret reduces to a difference in performance attributable to the oracle’s use of  $\mathbf{X} = \mathbf{O} \setminus (\mathbf{Z} \cup \mathbf{W})$ . Note that in the linear case, counterfactuals take the form of *auxiliary variables* (AVs) (Chen et al., 2016, 2017): modifications of observed variables in which the effects of some (or all) observed parents are removed. For example, in Fig 3a we have the AV  $Z^* = Z - \lambda_{xz}X$  which subtracts out the effect of  $X$  on  $Z$ . With respect to  $Z^*$ , the edge  $X \rightarrow Z$  is effectively removed. Thus,  $P(Y|Z^*)$  is the optimal stable predictor since any additional conditioning would activate unstable edge  $\lambda_{yx}$ .

**Theorem 5.** *For mean zero linear Gaussian SCMs, the MSE of a stable predictor is constant across environments.*

**Theorem 6.** *Let  $\mathcal{G}_0$  be the environment in which the coefficients associated with the unstable edges  $E_u$  are all zero. In  $\mathcal{G}_0$ , the MSE of the oracle predictor  $E_{\mathcal{G}_0}[Y|\mathbf{O}]$  is equal to the MSE of the optimal stable predictor  $E_{\mathcal{G}_0}[Y|\mathbf{Z}, \mathbf{W}^*]$ .*

We have established when the stable MSE is equal to the oracle MSE and that the performance of a stable predictor is a constant baseline across environments. The next result identifies environments for which the oracle MSE is lowest (and thus maximally different from the stable MSE).

**Lemma 7.** *Suppose there is only one unstable edge  $e$  with corresponding coefficient  $\lambda$  and that this edge is active for the oracle predictor. As  $|\lambda| \rightarrow \infty$  we have that the oracle MSE  $\rightarrow 0$ .*

To visualize these results in the context of example Fig 3a, in Fig 3b we plot the MSE of the oracle predictor (blue) and stable predictor  $E[Y|Z^*]$  (green) as we vary the strength of the unstable edge  $\lambda_{yx}$ . As we expect, the gap between the stable and oracle MSEs increases with the strength of the unstable edge. As a result, we lose the most information when the unstable association is strongest.

The figure also demonstrates an important performance consequence of stable predictors. **Key Result:** There is a *stability-performance tradeoff* between stability (and the ability to generalize well to new environments) and the performance in and near the training environment. In Fig 3b the performance of the unstable predictor (red)  $E[Y|X, Z]$  is better than the performance of the stable predictor for a range of environments corresponding to an interval (denoted by vertical dashed lines) surrounding the training value  $\lambda_{yx} = 5$ . Beyond this value, the unstable predictor’s performance significantly and rapidly deteriorates, demonstrating poor generalization under large shifts. More generally, the results in Fig 3b provide a useful visual characterization of the performance of stable and unstable predictors that makes it easy to reason about edge strengths, which we can learn from data, and can help us decide which invariances will be beneficial to enforce.

## 5 Trading Off Stability vs Performance Under Uncertainty

### 5.1 When Are Unstable Edges Beneficial?

We have just seen that there is a stability-performance tradeoff, since deleting edges incurs performance regret in nearly every environment. This is the consequence of minimizing worst-case (minimax) loss (Berger, 2013), in which case the constant performance of a stable predictor is optimal. We also saw that unstable predictors (e.g., red curve in Fig 3b) outperform stable predictors for finite deviations from the source environment. Thus, given a stable predictor, reincorporating unstable edges can be beneficial on the basis of environments we expect to see. In the following



---

**Algorithm 1:** Stepwise Instability Reincorporation

---

**input** : Prior  $P(\theta)$ , Features  $\mathbf{W}^* \cup \mathbf{Z}$ , Remaining features  $\mathbf{X}$ , Covariance  $\Sigma(\theta)$ **output**: New feature set $\mathbf{F} = \mathbf{W}^* \cup \mathbf{Z}$ ; **while**  $\mathbf{X} \neq \emptyset$  and adding features to  $\mathbf{F}$  lowers  $\hat{E}_{P(\theta)}[MSE]$  **do**    Find  $X \in \mathbf{X}$  that most lowers  $\hat{E}_{P(\theta)}[MSE]$ ;     $\mathbf{F} = \mathbf{F} \cup \{X\}$ ;  $\mathbf{X} = \mathbf{X} \setminus \{X\}$ ;**return**  $\mathbf{F}, \beta_{Y,\mathbf{F}}$ 

---

simulation, we show how incorporating unstable edges affects average and worst-case performance for varying priors over possible target environments.

Given a stable predictor, one can place a prior over possible environments  $P(\theta)$  and reinclude unstable edges that minimize the expected risk across probable environments:  $E_{\theta}[MSE]$ . Given two sets of regression weights  $\beta_1, \beta_2$  (e.g., one corresponding to a stable predictor), we can choose between them by Monte Carlo sampling possible environments and computing the average MSE using Eq 1, where  $e_y$  is a one-hot vector (1 for  $Y$  and 0 for other vars in  $\mathbf{O}$ ) and the target environment's covariance matrix is  $\Sigma = \Sigma(\theta)$ :

$$MSE(\beta) = E[(Y - \hat{Y})^2] = e_y^T \Sigma e_y - 2\beta^T \Sigma e_y + \beta^T \Sigma \beta \quad (1)$$

This procedure lets us add unstable associations back into a stable predictor in a stepwise fashion (Alg 1). Recalling that in addition to the features used by a level 3 stable predictor ( $E[Y|\mathbf{W}^*, \mathbf{Z}]$ ), an oracle predictor uses factual variables  $\mathbf{X} = \mathbf{O} \setminus (\mathbf{Z} \cup \mathbf{W})$ , we can consider reincorporating them into the feature set so long as they reduce the expected risk. By applying this algorithm to environments drawn from varying priors we can examine how adding unstable edges results in a tradeoff between average regret across environments and worst-case loss.

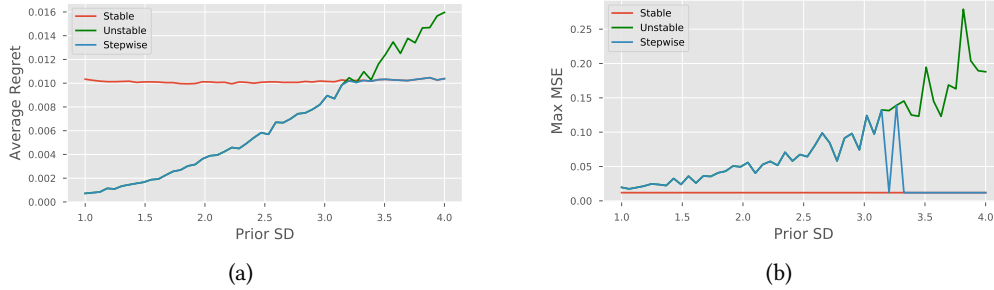


Figure 4: (a) Average regret and (b) minimax MSE for increasingly diffuse priors over environments.

Using the example from Fig 3a, we demonstrate how varying uncertainty in target environment 1) affects the decision to reinclude unstable associations on the basis of average performance and 2) the corresponding affect on worst-case loss. We posit a normal prior over the unstable edge coefficient centered at its source environment value and consider what happens as we increase the prior's standard deviation  $\sigma$ , representing less certainty in the similarity of possible environments. We apply Algorithm 1 and compare the average regret and worst-case MSE associated with stable, unstable, and stepwise unstable predictors as assessed by 1000 samples from each prior.

The results (plotted in Fig 4) demonstrate a clear tradeoff between local (average regret) and global (minimax MSE) performance. While for the bottom 66% of the priors ( $\sigma < 3.1$ ) the unstable predictor has lower average regret, *it has a worse max MSE for all priors considered*. The stepwise predictor, which uses an average performance decision rule, inherits the worse max MSE performance of the unstable predictor for  $\sigma < 3.3$ . Thus, this experiment shows that the optimality of stable predictors is closely tied to the choice of performance metric and degree of uncertainty. **Key Result:** *When we are concerned about the worst-case or when there is high variability in the possible environments, using only stable information to predict will be preferable*. For other cases this motivates future work on how to optimally incorporate unstable associations.



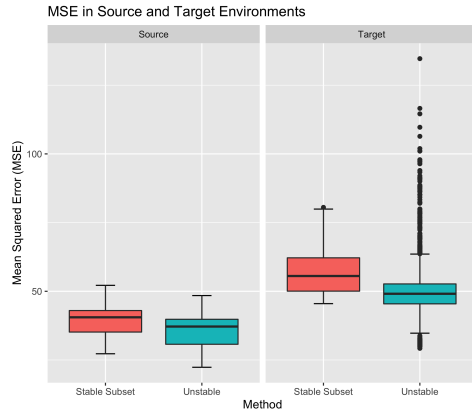


Figure 5: MSEs of an unstable regression using all features (blue) vs a stable subset (red) in environments (defined by season). The subplots indicate if the model is being evaluated on Source or Target data.

## 5.2 Measuring Stability-Performance Tradeoff in Real Data

Using real data, we now ask how does the stability-performance tradeoff manifest in non-linear settings? Specifically, we use the UCI Bike Sharing dataset (Fanaee-T and Gama, 2013) which has been previously used to investigate shifts in environment (Rothenhäusler et al., 2018; Subbaswamy et al., 2019). It contains 17,379 examples of hourly weather data measurements (temperature, feeling temperature, wind speed, and humidity) over the course of two years. The goal is to predict the number of hourly bike rentals (transformed from count to continuous variable by taking the square root). To define different environments we split the data by season such that the environments will differ in weather patterns and bike rental habits. We took each season in turn as the source environment, and evaluated predictive performance in terms of mean squared error (MSE) on heldout source data (from an 80/20 train/test split) and the full data of each of the three target environments. For each source environment, we repeated the train/test split 100 times.

Since our goal is to demonstrate the stability performance tradeoff, we consider two models: an unstable model which does not account for shifts in environment and a stable model. Because we do not know the graph of the underlying DGP for this dataset, we used a dataset-driven method (Rojas-Carulla et al., 2018) on held-out data from all environments to determine a stable feature subset (i.e., a level 1 distribution). The invariant feature subset returned consisted of ‘Humidity’ and ‘Windspeed’. We trained the stable and unstable models using Random Forest regressors (default scikit-learn (Pedregosa et al., 2011) parameters).

Boxplots of the performance of the stable and unstable models in Source and Target environments are shown in Fig 5. In the left panel, the unstable model (blue) slightly outperforms the stable model when evaluated in the source environment (median MSE of 37 vs 41). As expected, unstable models retain unstable information that improves performance in the source environment. When evaluated in the target environments (right panel), we make two interesting observations: First, the unstable model has highly varying performance in target environments, with a range of 105 as opposed to the stable model which has a range of 35 for target environment MSEs. Second, on average, the unstable model has lower error (average MSE 51) than the stable model (average MSE 58) in target environments. This shows that, in the worst case, the performance of the unstable model in the target environment can be extremely poor, but that for the “typical” target environment, the unstable model outperforms the stable model. This agrees with our findings in Section 5.1 and Fig 3b and shows that, *even in non-linear settings, the degree to which stability is desirable depends on how concerned we are about large shifts*. For example, in safety-critical domains optimizing against worst-case shifts may be more sensible than in other domains.

## 6 Conclusion

The use of machine learning in production represents a shift from applying models to static datasets to applying them in the real world. As a result, aspects of the underlying DGP are almost certain

to change. Many methods have been developed to find distributions that are stable to shifts in environment, but they have been expressed in differing languages and consider different types of shifts, making it difficult to compare them. To address this, we developed a framework for expressing the different types of shifts as unstable edges in a graphical representation of the DGP. Through a universal hierarchy of stable distributions, we established when and how stability can be achieved, allowing existing and future methodological work to be compared within the same framework. The hierarchy motivates future work on finding and estimating interventional and counterfactual distributions to determine when we can remove only the unstable edges, thereby giving us an optimal stable model. Regarding performance, we showed that there is a tradeoff between stability and average performance. Thus, while stability has benefits with respect to worst-case loss, future work may more closely examine how to balance between worst-case and expected performance.

## References

- Dario Amodei, Chris Olah, Jacob Steinhardt, Paul Christiano, John Schulman, and Dan Mané. Concrete problems in ai safety. *arXiv preprint arXiv:1606.06565*, 2016.
- James O Berger. *Statistical decision theory and Bayesian analysis*. Springer Science & Business Media, 2013.
- Rich Caruana, Yin Lou, Johannes Gehrke, Paul Koch, Marc Sturm, and Noemie Elhadad. Intelligible models for healthcare: Predicting pneumonia risk and hospital 30-day readmission. In *Proceedings of the 21th ACM SIGKDD International Conference on Knowledge Discovery and Data Mining*, pages 1721–1730. ACM, 2015.
- Bryant Chen, Judea Pearl, and Elias Bareinboim. Incorporating knowledge into structural equation models using auxiliary variables. In *Proceedings of the Twenty-Fifth International Joint Conference on Artificial Intelligence*, pages 3577–3583. AAAI Press, 2016.
- Bryant Chen, Daniel Kumor, and Elias Bareinboim. Identification and model testing in linear structural equation models using auxiliary variables. In *Proceedings of the 34th International Conference on Machine Learning-Volume 70*, pages 757–766. JMLR. org, 2017.
- Gregory F Cooper, Constantin F Aliferis, Richard Ambrosino, John Aronis, Bruce G Buchanan, Richard Caruana, Michael J Fine, Clark Glymour, Geoffrey Gordon, Barbara H Hanusa, et al. An evaluation of machine-learning methods for predicting pneumonia mortality. *Artificial intelligence in medicine*, 9(2):107–138, 1997.
- Hadi Fanaee-T and Joao Gama. Event labeling combining ensemble detectors and background knowledge. *Progress in Artificial Intelligence*, pages 1–15, 2013.
- Jerome Friedman, Trevor Hastie, and Robert Tibshirani. *The elements of statistical learning*, volume 1. Springer series in statistics New York, 2001.
- Christina Heinze-Deml and Nicolai Meinshausen. Conditional variance penalties and domain shift robustness. *arXiv preprint arXiv:1710.11469*, 2017.
- Christina Heinze-Deml, Jonas Peters, and Nicolai Meinshausen. Invariant causal prediction for nonlinear models. *Journal of Causal Inference*, 6(2), 2018.
- Katharine E Henry, David N Hager, Peter J Pronovost, and Suchi Saria. A targeted real-time early warning score (trewscore) for septic shock. *Science translational medicine*, 7(299):299ra122–299ra122, 2015.
- Kun Kuang, Peng Cui, Susan Athey, Ruoxuan Xiong, and Bo Li. Stable prediction across unknown environments. In *Proceedings of the 24th ACM SIGKDD International Conference on Knowledge Discovery & Data Mining*, pages 1617–1626. ACM, 2018.
- Kristian Lum and William Isaac. To predict and serve? *Significance*, 13(5):14–19, 2016.
- Sara Magliacane, Thijs van Ommen, Tom Claassen, Stephan Bongers, Philip Versteeg, and Joris M Mooij. Domain adaptation by using causal inference to predict invariant conditional distributions. In *Advances in Neural Information Processing Systems*, pages 10869–10879, 2018.

- Nicolai Meinshausen. Causality from a distributional robustness point of view. In *2018 IEEE Data Science Workshop (DSW)*, pages 6–10. IEEE, 2018.
- Judea Pearl. *Probabilistic Reasoning in Intelligent Systems: Networks of Plausible Inference*. Morgan Kaufmann, 1988.
- Judea Pearl. *Causality*. Cambridge university press, 2009.
- Judea Pearl and Elias Bareinboim. Transportability of causal and statistical relations: a formal approach. In *Proceedings of the Twenty-Fifth AAAI Conference on Artificial Intelligence*, pages 247–254. AAAI Press, 2011.
- Fabian Pedregosa, Gaël Varoquaux, Alexandre Gramfort, Vincent Michel, Bertrand Thirion, Olivier Grisel, Mathieu Blondel, Peter Prettenhofer, Ron Weiss, Vincent Dubourg, et al. Scikit-learn: Machine learning in python. *Journal of machine learning research*, 12(Oct):2825–2830, 2011.
- Jonas Peters, Peter Bühlmann, and Nicolai Meinshausen. Causal inference by using invariant prediction: identification and confidence intervals. *Journal of the Royal Statistical Society: Series B (Statistical Methodology)*, 78(5):947–1012, 2016.
- Jonas Peters, Dominik Janzing, and Bernhard Schölkopf. *Elements of causal inference: foundations and learning algorithms*. MIT press, 2017.
- J Quiñero-Candela, Masashi Sugiyama, Anton Schwaighofer, and Neil D Lawrence. Dataset shift in machine learning, 2009.
- Mateo Rojas-Carulla, Bernhard Schölkopf, Richard Turner, and Jonas Peters. Invariant models for causal transfer learning. *The Journal of Machine Learning Research*, 19(1):1309–1342, 2018.
- Dominik Rothenhäusler, Nicolai Meinshausen, Peter Bühlmann, and Jonas Peters. Anchor regression: heterogeneous data meets causality. *arXiv preprint arXiv:1801.06229*, 2018.
- Suchi Saria and Adarsh Subbaswamy. Tutorial: Safe and reliable machine learning. In *ACM Conference on Fairness, Accountability, and Transparency (FAT\*)*. ACM, 2019.
- Peter Schulam and Suchi Saria. Reliable decision support using counterfactual models. In *Advances in Neural Information Processing Systems*, pages 1697–1708, 2017.
- Ilya Shpitser and Eric Tchetgen Tchetgen. Causal inference with a graphical hierarchy of interventions. *Annals of statistics*, 44(6):2433, 2016.
- Aman Sinha, Hongseok Namkoong, and John Duchi. Certifying some distributional robustness with principled adversarial training. *arXiv preprint arXiv:1710.10571*, 2017.
- Peter Spirtes, Clark N Glymour, Richard Scheines, David Heckerman, Christopher Meek, Gregory Cooper, and Thomas Richardson. *Causation, prediction, and search*. MIT press, 2000.
- Adarsh Subbaswamy and Suchi Saria. Counterfactual normalization: Proactively addressing dataset shift using causal mechanisms. In *Uncertainty in Artificial Intelligence*, 2018.
- Adarsh Subbaswamy, Peter Schulam, and Suchi Saria. Preventing failures due to dataset shift: Learning predictive models that transport. In *Artificial Intelligence and Statistics (AISTATS)*, 2019.
- Kun-Hsing Yu, Andrew L Beam, and Isaac S Kohane. Artificial intelligence in healthcare. *Nature biomedical engineering*, 2(10):719, 2018.

## A Proofs

**Theorem 1.**  $P(Y|Z)$  is stable if there is no active unstable path from  $Z$  to  $Y$  in  $\mathcal{G}$  and the mechanism generating  $Y$  is stable.

*Proof.* We first translate our unstable edge representation of the graph to the selection diagram (Pearl and Bareinboim, 2011) representation used by Subbaswamy et al. (2019). For an edge  $e$  let  $He(e)$  denote the variables that  $e$  points into. Now for each  $e \in E_u$ , add a unique selection variable that points to each  $V = He(e)$ . This indicates that the mechanism that generates  $V$  is unstable. From Definition 3 in Subbaswamy et al. (2019) we know that a distribution is stable if  $S \perp\!\!\!\perp Y$ .

There are two possible ways there can be an active path from a variable  $S \in \mathbf{S}$  to  $Y$ . If there is an active forward path from  $S$  to  $Y$  (e.g.,  $S \rightarrow ch(S) \rightarrow \dots Y$ ) then there is a corresponding active path from  $Ta(e)$  to  $Y$  that contains the unstable edge  $e$  (e.g.,  $Ta(e) - e \rightarrow ch(S) \rightarrow \dots Y$ ). An active forward path can also indicate that the mechanism that generates  $Y$  is unstable.

Alternatively, if there is an active collider path from  $S$  to  $Y$  (e.g.,  $S \rightarrow ch(S) \leftarrow \dots Y$ ) then there is a corresponding active path from  $He(e) = ch(S)$  to  $Y$  that contains  $e$  (e.g.,  $Ta(e) - e \rightarrow ch(S) \leftarrow \dots Y$ ). Thus, in the selection diagram representation if  $P(Y|Z)$  is unstable then there is an active unstable path from  $Z \in \mathbf{Z}$  to  $Y$  since it means  $Y \not\perp\!\!\!\perp S|Z$ . Taking the contrapositive of this statement proves the theorem.  $\square$

**Lemma 3** (Subbaswamy et al. (2019), Corollary 1). A stable level 1 distribution of the form  $P(Y|Z)$  can be expressed as a stable level 2 distribution of the form  $P(Y|Z', do(\mathbf{W}))$  for  $Z' \subseteq \mathbf{Z} \subseteq \mathbf{O}$ ,  $\mathbf{W} \subseteq \mathbf{O}$ .

*Proof.* This is a restatement of Corollary 1 in Subbaswamy et al. (2019).  $\square$

**Lemma 4.** A stable level 2 distribution of the form  $P(Y|Z', do(\mathbf{W}))$  can be expressed as a stable level 3 distribution of the form  $P(Y(\mathbf{W})|Z'(\mathbf{W}))$ .

*Proof.* Consider the (level 2) intervention  $do(X) = x$ . For a variable  $V$  letting  $V(x)$  denote the value  $V$  would have taken had  $X$  been set to  $x$  we have that  $P(V(x)) = P(V|do(x))$ . When interventions are consistent (i.e., for  $x \neq x'$  there are no conflicting interventions  $do(X = x)$  and  $do(X = x')$ ) counterfactuals reduce to the *potential responses* of interventions expressible with the *do* operator (Pearl, 2009, Definition 7.1.4).  $\square$

**Theorem 5.** For mean zero linear Gaussian SCMs, the MSE of a stable predictor is constant across environments.

*Proof.* First, recall that for a feature set  $Z$ , asymptotically (as sample size becomes infinite)  $MSE = E[Var(Y|Z)]$ . We know a stable predictor models a stable distribution of the form  $P(Y|Z, \mathbf{W}^*)$ , where  $\mathbf{W}^*$  consists of AVs (i.e., counterfactuals). For any two environments  $\mathcal{G}_1, \mathcal{G}_2$  which are instantiations of the graph  $\mathcal{G}$ , stability yields the following:

$$P_1(Y|Z, \mathbf{W}^*) = P_2(Y|Z, \mathbf{W}^*) \implies Var_1(Y|Z, \mathbf{W}^*) = Var_2(Y|Z, \mathbf{W}^*).$$

Further, for centered multivariate Gaussians (recall we assumed all variables are mean 0)  $Var(Y|X = \mathbf{x}) = Var(Y|X)$  such that conditional variance is constant for all values of the conditioned variables. Thus,  $MSE = E[Var(Y|Z, \mathbf{W}^*)] = Var(Y|Z, \mathbf{W}^*)$  is the same in  $\mathcal{G}_1$  and  $\mathcal{G}_2$ .  $\square$

**Theorem 6.** Let  $\mathcal{G}_0$  be the environment in which the coefficients associated with the unstable edges  $E_u$  are all zero. In  $\mathcal{G}_0$ , the MSE of the oracle predictor  $E_{\mathcal{G}_0}[Y|O]$  is equal to the MSE of the optimal stable predictor  $E_{\mathcal{G}_0}[Y|Z, \mathbf{W}^*]$ .

*Proof.* First, note that a coefficient value of zero is equivalent to deleting an edge. If it is a directed edge, it corresponds to a 0 entry in the structural coefficient matrix  $\Lambda$ . If it is a bidirected edge then it corresponds to a 0 entry in the off-diagonal of the covariance matrix  $\mathcal{E}$  of the exogenous variables.

Graphically, the effect of the *do* operator is to delete the edges into the variables that are intervened upon (i.e.,  $do(X)$  corresponds to the graph  $\mathcal{G}_{\bar{X}}$  (Pearl, 2009)). Thus, if we let  $\mathbf{V} \subseteq \mathbf{O}$  be the variables with unstable edges into them, and  $\mathbf{U} = \mathbf{O} \setminus \mathbf{V}$ , then the environment  $\mathcal{G}_0$  is exactly an environment in which  $P_0(Y|O) = P(Y|U, do(\mathbf{V}))$ . Next, by Lemma 4 we know the conditional interventional

distribution can be equivalently expressed in the form  $P(Y|Z, \mathbf{W}^*)$ . Since  $P_0(Y|\mathbf{O}) = P(Y|Z, \mathbf{W}^*)$ , we have that  $\text{Var}_0(Y|\mathbf{O}) = \text{Var}(Y|Z, \mathbf{W}^*)$  and thus the MSEs are equal.  $\square$

**Lemma 7.** *Suppose there is only one unstable edge  $e$  with corresponding coefficient  $\lambda$  and that this edge is active for the oracle predictor. As  $|\lambda| \rightarrow \infty$  we have that the oracle MSE  $\rightarrow 0$ .*

*Proof.* Sketch: Reduce this by considering predicting  $Y$  from a single variable  $X$  (transform the graph after marginalizing and conditioning over the other variables). For linear Gaussian SCMs we have that  $E[Y|X]$  is of the form  $aX + b$ . Thus,  $R^2 = \rho_{xy}^2$ , and it suffices to show that  $\lim_{|\lambda| \rightarrow \infty} \rho_{xy}^2 = 1$ .  $\square$

## B Simulation Experiment Details

### B.1 Details

We generated the linear SCMs parameters as follows:

```
import numpy as np

lyx = np.random.uniform(2, 4) * (2 * np.random.binomial(1, 0.5) - 1)
lyz = np.random.uniform(0.1, 2) * (2 * np.random.binomial(1, 0.5) - 1)
lxz = np.random.uniform(0.1, 2) * (2 * np.random.binomial(1, 0.5) - 1)
v = 0.1 ** 2
```

where  $v$  is the variance of the exogenous noise variables. We generated 10,000 training data points and considered 50 increments of the prior standard deviation  $\sigma$  from 1 to 4. To estimate the AV  $Z^*$  we used the estimated coefficient  $\hat{\lambda}_{xz}$  learned from training data.

## C Bikesharing Experiment

Following Rothenhäusler et al. (2018) we use the UCI Bike Sharing dataset (Fanaee-T and Gama, 2013) in which the goal is to predict the number of hourly bike rentals  $R$  from weather data including temperature  $T$ , feeling temperature  $F$ , wind speed  $W$ , and humidity  $H$ . As in Rothenhäusler et al. (2018), we transform  $R$  from a count to continuous variable using the square root. The data contains 17,379 examples with temporal information such as season and year.

Subbaswamy et al. (2019) posited the graph in Fig 6, in which all mechanisms except for  $R$  varied. When we applied their estimator to the month-based split it exhibited highly unstable performance which indicates their hypothesized graph or mechanism shift may not hold. Further, based on the unstable performance of all estimators tried, we believe the mechanism that generates the bike rentals  $R$  likely varies across environments. This instability will only be magnified by model misspecification.

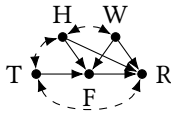


Figure 6: Posited graph from Subbaswamy et al. (2019).

For this reason we turned to Causal transfer learning (CT) Rojas-Carulla et al. (2018) which searches for invariant subsets. The algorithm hyperparameters dictating how much data to use for validation, the significance level, and which hypothesis test to use. In all experiments we set `valid_split = 0.5`, `delta=0.3`, and `use_hsic = False` (using HSIC always returned the full feature set). We considered various subsets returned by the algorithm of Rojas-Carulla et al. (2018), the one plotted in the main paper was the subset which performed the best on a 20% dev holdout. This subset was Humidity and Windspeed.